

PACS numbers: 43.35.Sx; 42.25.Dd
DOI: 10.1070/QE2006v036n12ABEH013261

Direct opto-acoustic *in vitro* measurement of the spatial distribution of laser radiation in biological media

I.M. Pelivanov, S.A. Belov, V.S. Solomatin, T.D. Khokhlova, A.A. Karabutov

***Abstract*. The problem of opto-acoustic (AO) diagnostics of light scattering and absorption in biological media is considered. The objects under study were milk, bovine and porcine liver, and bovine muscle tissue. The forward and backward schemes for recording acoustic signals were used in experiments. The spatial distribution of the light intensity was measured for each biological medium from the temporal profile of the excited OA pulse and the absorption coefficient and reduced scattering coefficient were determined. Opto-acoustic signals were excited by a 1064-nm pulsed Nd : YAG laser and a tunable Ti : sapphire laser at 779 nm. It is shown that the proposed method can be used for obtaining *a priori* information on a biological medium in problems of optical and AO tomography.**

Keywords: *optics of biological tissues, absorption coefficient, scattering coefficient, laser opto-acoustics.*

1. Introduction

During the past decade, lasers are finding increasing applications in various problems of diagnostics of biological tissues and media [1]. Optical methods are obviously attractive because of their noninvasive nature. A significant place among them is occupied by the methods for visualisation of absorbing inhomogeneities such as optical [2 – 4] and opto-acoustic (OA) [5 – 11] tomography. The contrast of images obtained by both these methods is determined by the difference in the absorption coefficients of inhomogeneities (for example, a malignant or benign tumour) and the surrounding tissue [2, 11].

Biological tissues are highly scattering in the visible and near-IR spectral regions [12]. This circumstance considerably reduces the possibilities of tomography by restricting the probe depth (the maximum distance from the medium surface to an inhomogeneity of one or other type at which it can be still detected) and the minimal size of objects that can be visualised. In addition, to determine the optimal wavelength and construct algorithms for solving inverse tomography problems, *a priori* data about the optical properties of tissues under study are required.

Therefore, the study of the distribution of laser radiation in turbid media remains an actual problem. Great recent progress in the *in vivo* measurements of optical characteristics of biological tissues was achieved by using backscattering methods such as scattering spectroscopy with the frequency [13 – 16], spatial [17, 18], and time [19 – 22] resolution.

Note that the time-resolved method is most developed among these methods. Measurements are based on the recording of the temporal profile of a picosecond laser pulse backscattered by a medium. Its time delay with respect to the reference (unscattered) pulse determines the scattering coefficient of the medium, while the exponential decay rate determines the absorption coefficient (see, for example, [19]). Therefore, the contributions of absorption and scattering are taken into account separately. Calculations are usually based on the diffusion approximation of the radiation transfer equation. Measurements can be conveniently performed by using radiation from a picosecond Ti : sapphire laser tunable between 600 and 1100 nm or radiation from several diode lasers emitting in the same spectral range. It was shown in [22] that these lasers can be used in clinics. The absorption and scattering spectra of main human tissues were obtained in [21, 23].

Despite numerous advantages of the methods considered above, they also have disadvantages. The main disadvantage is the assumption about the homogeneity of a medium used in calculations. Already in the case of a two-layer medium, significant, virtually insurmountable difficulties appear in the reconstruction of its optical properties [24]. The profile of a signal scattered by the medium does not have drastic distortions caused by the presence of layers or inhomogeneities. Therefore, the calculated optical coefficients contain only some integral information about the medium.

Thus, the local and direct measurement of the laser radiation distribution in biological media is still of current interest. This problem can be partially solved by using an optical coherence tomograph [25 – 27] that provides images with a spatial resolution of 5 – 20 μm. However, the probe depth is restricted in this case by strong scattering of light and is no more than 2 – 3 mm.

The OA method is based on the local thermooptic excitation of acoustic signals in a medium absorbing laser pulses. In the case of excitation by nanosecond laser pulses, the heat diffusion within the duration of the laser pulse can

I.M. Pelivanov, S.A. Belov, V.S. Solomatin, T.D. Khokhlova, A.A. Karabutov International Laser Center, M.V. Lomonosov Moscow State University, Vorob'evy gory, 119992 Moscow, Russia; e-mail: pelivanov@ilc.edu.ru, t_khokhlova@ilc.edu.ru

Received 25 May 2006; revision received 5 July 2006
Kvantovaya Elektronika **36** (12) 1089 – 1096 (2006)
Translated by M.N. Sapozhnikov

be neglected. If the laser-beam width exceeds the characteristic penetration depth μ_{eff}^{-1} of light into the medium [where $\mu_{\text{eff}}=(3\mu_a\mu_s')^{1/2}$ is the effective attenuation coefficient, and μ_a and μ_s' are the absorption coefficient and reduced scattering coefficient, respectively], the OA pulse profile repeats the in-depth distribution of the heat release, i.e. the spatial distribution of the absorbed radiation intensity. At present the OA microscopy [5, 28, 29] and tomography [9, 10, 30] methods are being developed and refined.

The authors of papers [31, 32] proposed to use the OA effect for direct measurements of the spatial distribution of laser radiation in scattering media and optical parameters of these media. It was shown that the optical properties of turbid media can be determined from the temporal shape of the excited OA pulse.

The aim of this paper was to demonstrate the use of the OA method developed in [32] for direct *in vitro* measurements of the spatial distribution of the light intensity in biological media and determining their optical properties.

2. Materials

It should be remembered in the study of biological objects that the sample preparation procedure and diagnostics itself can cause irreversible changes in samples. During *in vitro* measurements of biological tissues, such changes always occur. To interpret adequately the results of OA measurements, we will describe below the preparation procedure of samples for OA studies.

All the tissues under study (bovine and porcine liver, and bovine muscle tissue) were stored for no more than 72 h after the slaughter and did not undergo any temperature processing (freezing, high-temperature heating). Samples of size 3×3 cm and thickness 2 cm were cut, which then were placed for some time into a vessel with distilled water. The vessel was slightly evacuated down to a pressure of about 0.5 atm. This procedure was performed to remove air bubbles from biological tissues, which strongly distort the temporal profile of OA signals excited in biological tissues. In this case, blood was also partially lost. Experiments were performed for several samples prepared from tissue of the same type but belonging to different animals, and also for different parts of the same sample. Table 1 presents the statistically averaged results of measurements.

The laser fluence E_0 incident on a sample in experiments was less than 3 and 10 mJ cm^{-2} at wavelengths 779 and 1064 nm, respectively, which is much lower than the safety threshold [33]. The heating of the medium produced by a laser pulse [34]

$$\Delta T \approx \frac{\mu_a E_0}{\rho c_p} \tag{1}$$

(where ρ and c_p are the density and heat capacity of the medium) was less than one hundredth of degree, and less than one degree for the entire measurement that included averaging over 128 signals. Thus, variations in the optical and thermal properties of media caused by laser irradiation could be neglected.

3. Opto-acoustic method

The arrangement of the transmitter and receiver in OA diagnostic setups can be different. In the forward mode, OA signals are excited and detected at the opposite sides of the medium under study, while in the backward mode, they are excited and detected at the same side. Below we consider and compare the experimental results obtained by using both detection modes.

3.1 Forward mode of OA signal detection

Figure 1 shows the diagram of the forward mode of OA signal detection. The medium under study is placed between a plate transparent for laser radiation, through which it is excited, and the surface of a broadband piezoelectric transducer. This provides the controllable thickness of the medium and the smoothness of its surfaces.

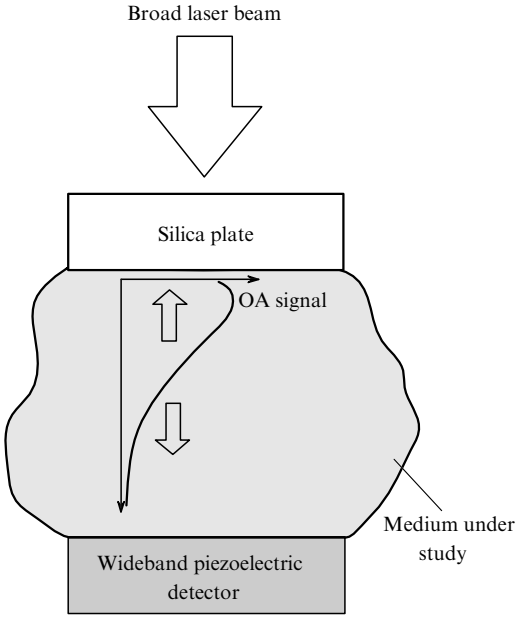

Figure 1. Principal scheme of the forward mode of OA signal detection.

The temporal profile of an OA signal excited in a non-heat-conducting medium (the length of heat diffusion within the duration of the laser pulse τ_L is much smaller than the light penetration depth $V_0\tau_L \gg \mu_{\text{eff}}^{-1}$) by a short laser pulse with the laser-beam diameter $d_0 \gg \mu_{\text{eff}}^{-1}$ can be written in the form [32, 34]

$$p_0(\tau = t - z/V_0) = \frac{\beta V_0^2}{2c_p}\mu_a E_0 \begin{cases} H(-V_0\tau), & \tau<0, \\ R_{\text{ac}}H(V_0\tau), & \tau>0, \end{cases} \tag{2}$$

where the z axis is directed inside from the medium boundary; $R_{\text{ac}} = (1-N)/(1+N)$ is the reflection coefficient of an ultrasonic wave from the scattering medium–transparent medium interface; N is the ratio of the acoustic impedances of the absorbing and transparent media; $H(z)$ is the spatial distribution of the light intensity in the medium; V_0 is the sound speed in the medium; and β is the coefficient of thermal expansion.

The leading edge of the OA signal $p_0(\tau < 0)$ repeats the spatial distribution of heat release and, as follows from (2), is proportional to the light intensity distribution $H(z)$ in the medium, the time scale of variations in $p_0(\tau)$ and the spatial scale of variations in $H(z)$ being related through the sound speed in the medium as $z = -V_0\tau$.

The specific feature of the distribution $H(z)$ in turbid media is that is has the maximum of the diffuse light intensity caused by multiple scattering at the subsurface layer at the distance $z_{max} \sim l^*$ from the medium boundary [31] (l^* is the photon transport free path in the medium). The intensity of this maximum can exceed the incident radiation intensity by a factor of 4–6.

In the case of an optically homogeneous scattering medium, the function $H(z)$ can be calculated numerically by the Monte-Carlo method [35, 36] from the known optical parameters (absorption coefficient μ_a, scattering coefficient μ_s, and anisotropy factor g), while at distances $z > (2 \div 3)l^*$, this function has the analytic form within the framework of a simple diffusion model [37]. There are also more rigorous solutions, for example, the P_3 or P_5 approximation in the solution of the radiation transfer equation [32].

By approximating the leading edge of an OA pulse at distances $z > (2 \div 3)l^*$ in a scattering medium by a theoretical dependence, the required optical parameters can be reconstructed [31]. For example, the effective attenuation coefficient $\mu_{eff} = (3\mu_a\mu_s')^{1/2}$ can be found from the exponential approximation of the leading edge of the OA pulse. The position of the maximum $z_{max} = -\tau_{max}V_0$ of the spatial distribution of the light intensity can be also determined only from the shape of the OA signal [31], i.e. without the absolute calibration of a pressure gauge. As shown in [32], the dependence of $z_{max}\mu_{eff}$ on μ_a/μ_{eff} in the range $0.05 < \mu_a/\mu_{eff} < 0.35$, which is typical for biological media and tissues, is universal and gives the empirical expression for measuring the absorption coefficient from experimental values of μ_{eff} and z_{max}:

$$\mu_a = -0.074\mu_{eff}\ln(1 - 3.62z_{max}\mu_{eff}). \quad (3)$$

Then, by using the expression $\mu_s' = \mu_{eff}^2/(3\mu_a)$, we can calculate the reduced scattering coefficient μ_s' in the medium. Note that this method for measuring z_{max} and μ_{eff} from the temporal profile of the OA signal can be used only in the forward mode of OA signal detection.

Thus, the method for studying the spatial distribution of the light intensity and determining optical coefficients in homogeneous turbid media was proposed in [31, 32] and tested in a model medium (suspension of titanium oxide particles in water) and milk. In this paper, we used this method for measurements in real biological media.

Opto-acoustic signals were excited by 10–12-ns pulses from a Q-switched 1064-nm Nd : YAG laser with a pulse repetition rate of 2 Hz or 30-ns, 779-nm pulses from a Ti : sapphire laser with a pulse repetition rate of 50 Hz. The main part of radiation passed through a light scatterer and a lens. This provided a nearly collimated beam with the uniform intensity distribution over its cross section, which ensured the one-dimensional geometry of measurements. The laser beam diameter on the medium surface was about 3 cm. A cell with a medium under study was covered with a silica glass. Opto-acoustic signals were detected with a broadband nonresonance piezoelectric transducer operating in the idling regime. A piezoelectric element was a polyvinyldenfluoride film of thickness 110 μm glued on a damping surface. The diameter of the piezoelectric element was 8 mm. This provided almost uniform sensitivity in the frequency range from 0.05 to 2 MHz equal to 845 μV Pa^{-1} after fifty-fold amplification. The minimal pressure of detected ultrasonic signals was several pascal and the dynamic range of the entire receiving system exceeded 40 dB. The acoustic signal transformed by the piezoelectric detector was recorded with a digital Tektronix TDS-220 oscilloscope.

Figures 2a and c show typical OA signals measured in experiments. For example, the OA signal recorded in milk has the bipolar shape, whereas, according to (1), it should have the unipolar profile. In reality, a broadband acoustic signal propagating in a medium experiences the diffraction transformation [34, 38]. Low frequencies are subjected to a stronger transformation than higher frequencies, which results in the distortion of the pulse shape. The effect of diffraction distortions can be eliminated analytically by using the expression [38]

$$p_0(\tau) = p_{exp}(\tau) + f_d\int_{-\infty}^{\tau} p_{exp}(t)dt, \quad (4)$$

where $p_{exp}(\tau)$ is the recorded signal; $f_d = 2V_0L/r^2$; r is the laser-beam radius on the medium surface; and L is the medium thickness. Another factor affecting the shape of the recorded signal is the nonuniformity of the spectral sensitivity of the detector at frequencies lower than 50 kHz.

In this paper, we reconstructed the initial shape of an OA pulse excited in a medium by using the deconvolution procedure, which consists in the following. Each time before measurements in a scattering medium, the response of the system to a signal from a strongly absorbing non-scattering probe medium is recorded (the spectral amplitude of this signal can be considered constant in the range from 0 to 2 MHz). In this case, excitation conditions, the acoustic properties and thickness of the probe medium should be the same as those for the scattering medium. Because factors distorting the pulse profile are 'linear', their influence on the probe-signal spectrum will be the same as that on the signal spectrum in the scattering medium. Therefore, after the deconvolution with the probe signal the influence of these factors will be eliminated.

Figure 2b shows the reconstructed initial profile of the OA pulse in the scattering medium. The OA signal before the deconvolution is shown in Fig. 2a. To obtain the probe signal from a strongly absorbing medium, we used the aqueous solution of black Indian ink. The absorption coefficient μ_a in it measured from the leading edge of the OA pulse was 320 cm^{-1}. For comparison, the absorption coefficient in milk at 1064 nm is 0.17 cm^{-1}, which is more than three orders of magnitude lower than μ_a in the black Indian ink solution; correspondingly, the range of excited ultrasonic frequencies is wider.

One can see from Figs 2a and b that the signal becomes unipolar after the deconvolution procedure, the amplitude ratio $A_2/A_1 = 0.76$ being coincident with the theoretical coefficient of reflection of an ultrasonic wave from the transparent medium–scattering medium interface [see (1)]. Extinction coefficients μ_{eff} determined from the approximation of the leading and trailing edges of the reconstructed pulse coincide within the experimental error. The value $z_{max} = V_0\tau_{max} = 0.052$, determined from the signal profile in Fig. 2b, was used for the calculation of the absorption coefficient by expression (3). The obtained value $\mu_a = 0.17 \pm 0.01$ cm^{-1} well agrees with the results of our previous paper [31]. This suggests that the reconstruction of the OA signal profile by the deconvolution method is correct.

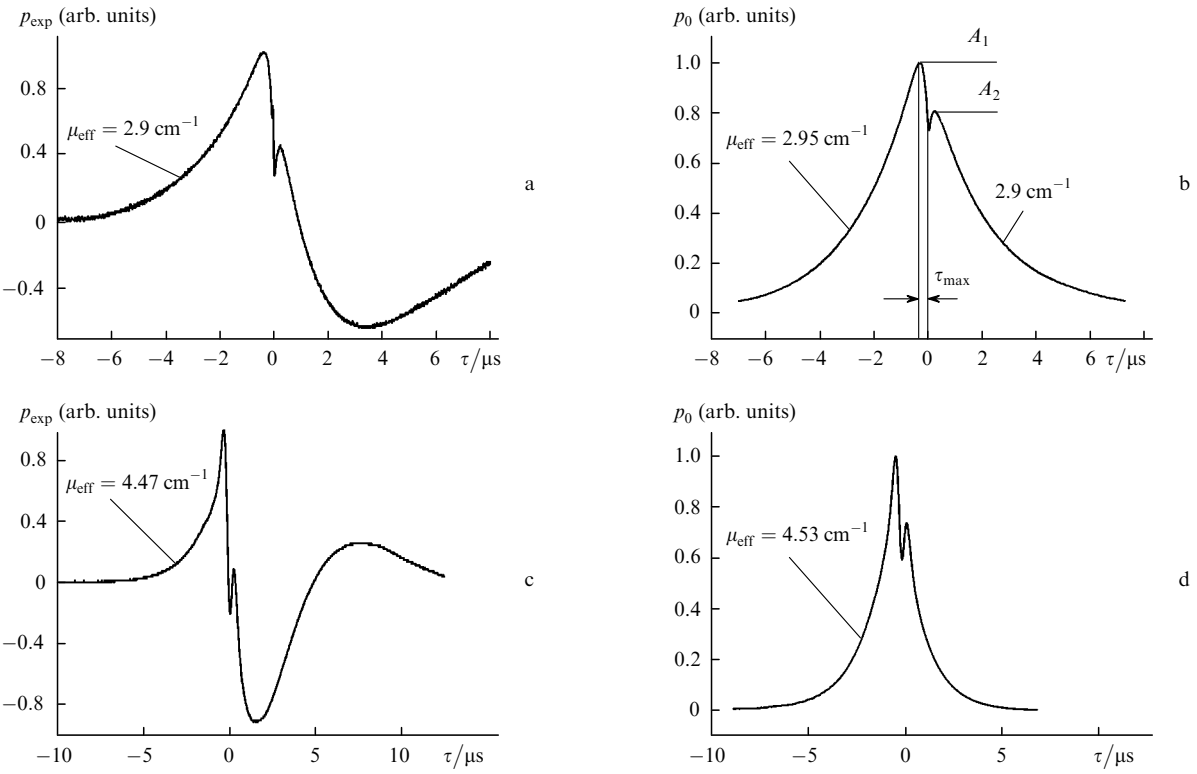

Figure 2. Typical temporal profiles of OA pulses recorded in milk (a) and porcine liver (b) and profiles of the corresponding reconstructed signals (b and d) in the same media after the deconvolution procedure.

Figures 2c and d show the OA signal profiles in porcine liver (recorded and obtained after the deconvolution, respectively) excited at a wavelength of 779 nm. One can see that the pulse profile is also reconstructed correctly. Similarly, we measured and processed OA signals in bovine liver and bovine muscle tissue excited at 779 and 1064 nm. The results of calculations of the optical properties of media studied in the paper are presented in Table 1.

An important characteristic of biological objects from the point of view of their optical diagnostics is the spatial distribution of the intensity of laser radiation intensity penetrated into the medium. As mentioned above, the leading edge of the OA signal repeats the spatial distribution of heat release in the medium, which allows the measurement of the local intensity distribution of laser radiation over depth. Figure 3 demonstrates at the logarithmic scale the spatial distributions of the laser radiation intensity in different media, which were constructed by using the OA signal profiles $p_0(\tau < 0)$ [see expression (2)]. The solid curves are the exponential approximations of the data obtained by the method of least squares.

3.2 Backward mode of OA signal detection

A substantial disadvantage of the forward mode of OA signal detection is that it requires the two-side access to an object under study. This makes the forward-mode detection too complicated to apply *in vivo* in most cases. The backward mode of OA signal detection is much more convenient and promising [39], and we consider below the possibility of its application for diagnostics of light scattering in biological objects.

Figure 4 shows the backward mode of OA signal detection. A collimated laser beam was directed from the side to a beamsplitter cube, which changed its propagation direction by 90°. At the top the cube was in contact with a medium under study and at the bottom with a wideband piezoelectric transducer. The cube was made of two triangle quartz prisms in optical contact, one of the touching surfaces being covered with a thin metal layer. An OA signal excited in the medium under study propagated through this layer without reflection losses and then was incident on a detector.

The absorption of the laser pulse in a sample is

Table 1.

Medium	Forward mode						Backward mode	
	μ_a/cm^{-1}		μ_s'/cm^{-1}		μ_{eff}/cm^{-1}		μ_a/cm^{-1}	
	1064 nm	779 nm	1064 nm	779 nm	1064 nm	779 nm	1064 nm	779 nm
Milk	0.17 ± 0.01	0.041 ± 0.002	17 ± 1	24 ± 1	2.90 ± 0.03	1.71 ± 0.03	–	–
Porcine liver	0.17 ± 0.05	0.36 ± 0.04	5 ± 5	18 ± 2	2.8 ± 0.2	4.4 ± 0.3	0.14 ± 0.02	0.44 ± 0.07
Bovine liver	0.11 ± 0.02	0.63 ± 0.07	23 ± 3	16 ± 2	2.7 ± 0.2	5.5 ± 0.3	0.13 ± 0.02	0.55 ± 0.09
Bovine muscle liver	0.15 ± 0.03	0.08 ± 0.01	12 ± 2	20 ± 3	2.3 ± 0.3	2.2 ± 0.2	0.15 ± 0.03	0.06 ± 0.01

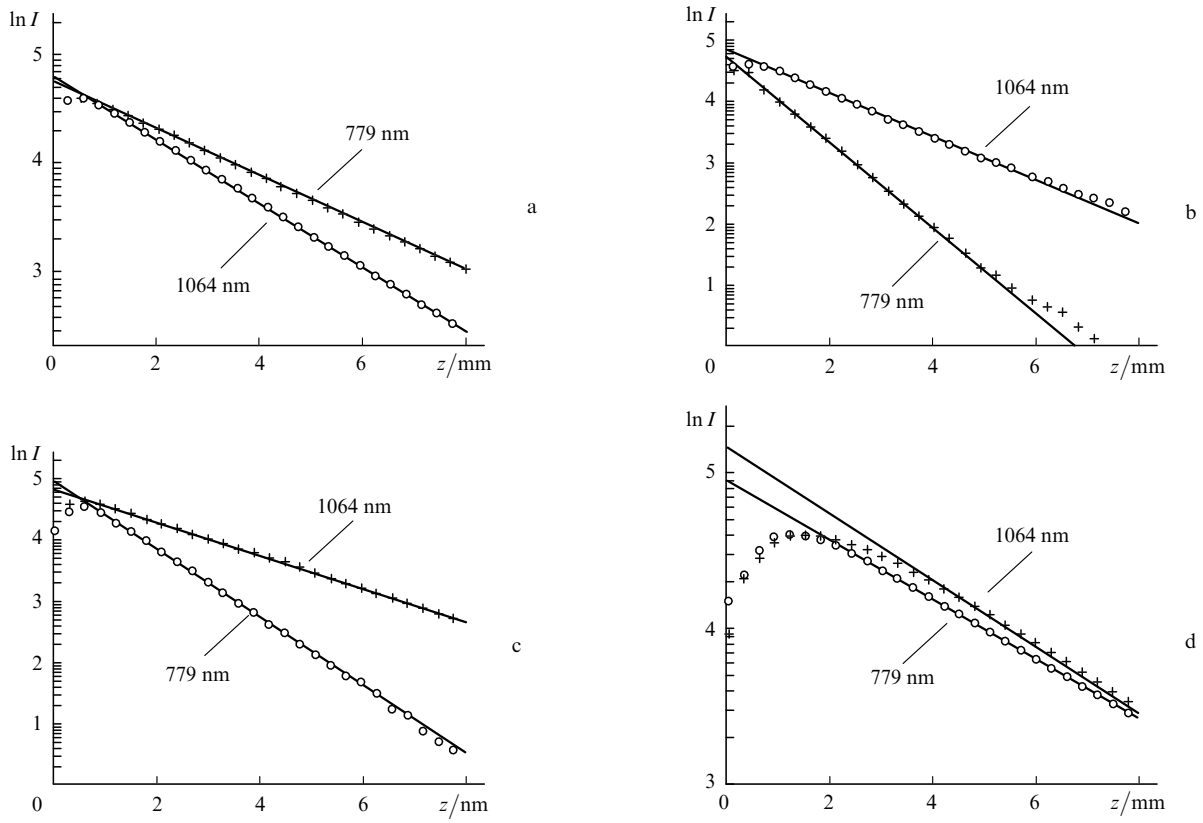

Figure 3. In-depth laser fluence distributions (in arb. units) in milk (a), porcine liver (b), bovine liver (c), and bovine muscle tissue (d).

accompanied by the appearance of two identical acoustic waves, the first wave propagating inside the medium and the second – in the opposite direction [34]. The temporal profile of the OA signal propagating to the detector (can be represented in the form

$$p_0(\tau = t - z/V_0) = \frac{\beta V_0^2}{2c_p}\mu_a E_0 \begin{cases} 0, & \tau<0, \\ R_{ac}H(V_0\tau), & \tau>0 \end{cases} \qquad (5)$$

by neglecting the influence of the laser-pulse duration and pulsed transient characteristic of the detector.

Taking into account the laser pulse duration, the OA signal profile is determined by the convolution of (5) with the time envelope of the laser pulse intensity and transient response of the piezoelectric detector. If the acoustic signal is recorded in the far-field diffraction zone, its temporal profile will correspond to the derivative of the shape of a signal excited at the boundary $z = 0$ [34].

Figure 5 presents OA signals obtained for different media in the backward mode. Measurements were performed in the far-field wave zone, and the laser-beam

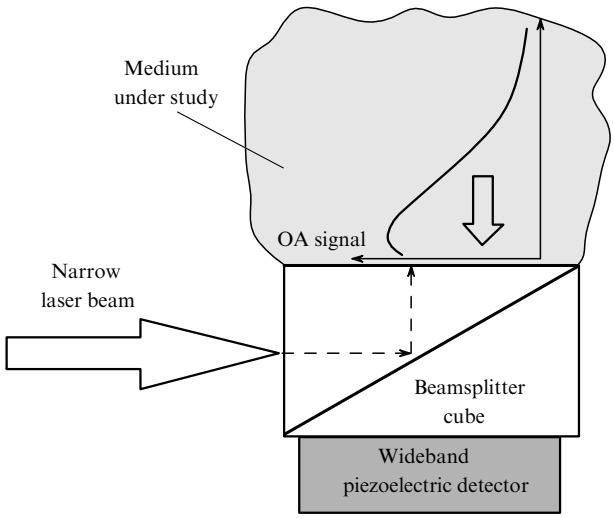

Figure 4. Principal scheme of the backward mode of OA signal detection.

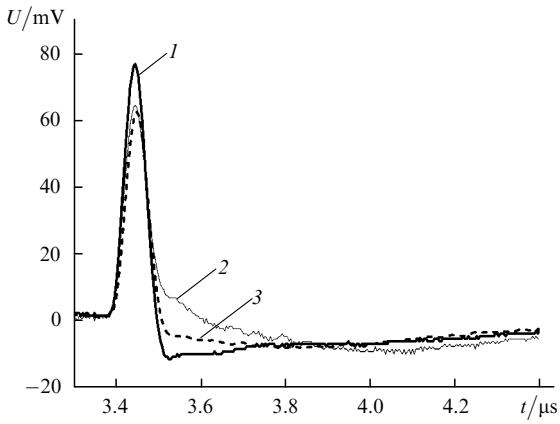

Figure 5. Typical OA signal profiles recorded with a piezoceramic detector in milk (*1*), porcine liver (*2*), and bovine muscle tissue (*3*) in the backward mode at 1064 nm.

diameter on the medium surface was 4 mm. Therefore, the width of a narrow positive peak in signals was determined by the width of the transient response of the detector, while its amplitude [according to (5)] was proportional to the absorption coefficient of the medium.

Thus, by comparing the amplitude of the OA signal excited in the medium under study with that of a signal obtained from the medium with the known absorption coefficient (for example, milk), we can determine the unknown absorption coefficient.

The results of diagnostics of light absorption in biological tissues obtained using the backward mode aare listed in Table 1.

4. Discussion

Let us now analyse in more detail the results obtained in the paper. We have considered the two main schemes of OA diagnostics of biological objects. Let us first of all compare them.

As shown in section 3.1, when the forward mode of OA signal detection is used, the leading edge of a pressure pulse repeats the in-depth distribution of laser fluence in the medium. This is extremely important because it can be used to estimate the optical homogeneity or inhomogeneity of an object being studied and calculate optical coefficients directly from the laser fluence distribution. Indeed, the description of a medium with the help of a set of optical coefficients is possible only when the medium is homogeneous, which is not always the case in real biological tissues. Any optical inhomogeneity located within the medium can introduce considerable errors in the calculation of volume – 'averaged' optical coefficients.

The laser fluence distributions presented in Fig. 3 were obtained for relatively homogeneous tissues. The laser fluence distribution in milk away from the boundary (Fig. 3a) has the universal exponential character. Note that OA measurements were performed for different samples of each type of tissue over ten times. Figures 3b – d present the laser fluence distributions for samples of bovine and porcine liver as well as bovine muscle tissue, these tissues having the best homogeneity. However, some deviations from the exponential approximation caused by the inhomogeneity of biological tissues are observed. Optical properties [light absorption, reduced scattering, and effective attenuation coefficients calculated from the in-depth laser fluence distributions (see Table 1)] are the result of statistical averaging over a set of more than ten samples. Despite the considerable possibilities of the method for *in vitro* diagnostics, the forward mode has substantial disadvantages. The basic disadvantage is the requirement of the two-side access to the object. In addition, samples should have a comparatively large thickness ($\sim$2 cm) to avoid the piezoelectric detector exposure, and the sample surface should be flat and plane – parallel. As a result, this method can be used for *in vivo* measurements only in special cases.

As shown in section 3.2, the backward mode of OA pulse detection permits measurements to be performed having just one-sided accesses to samples. This measurement method is much more convenient and can be used for *in vivo* diagnostics. However, the direct measurement of the spatial distribution of laser fluence in the case of the backward mode of OA signal detection involves severe difficulties. Unlike the forward mode, where the leading edge of the OA signal repeats the spatial distribution of heat release [see expression (2)], in this case, according to (5), information is contained in the trailing edge of the pulse. However, the pulse is subjected to a strong diffraction transformation [34, 38], while the reconstruction of the undistorted profile with the help of the deconvolution with a signal from a strongly absorbing medium does not give good results due to a small amplitude of spectral components containing this information. Nevertheless, the amplitude of an OA pulse excited in a scattering medium and recorded in the far-field diffraction zone is proportional to the absorption coefficient. Therefore, it can be measured in strongly scattering media by using the backward mode of the OA signal detection.

The optical properties of biological tissues calculated from our experimental data are presented in Table 1. Note first that the absorption coefficients of these tissues determined in different experimental geometries coincide within the experimental error, thus confirming the adequacy of the obtained results.

The absorption coefficient of the biological tissues at the Nd : YAG laser wavelength (1064 nm) proved to be close to the absorption coefficient of water. It seems that the differences in their values are related to the percentage of water in these tissues. Indeed, the absorption spectrum of a biological medium can be calculated from a linear combination of the spectra of its components: fats, proteins, blood, and water [19, 20, 22]. Proteins almost do not absorb light in the visible and near-IR regions [19]. The neglect of the absorption of light by fat tissue in calculations can lead to errors; however, the main absorbers in biological media are water and blood. Their percentage in a biological tissue mainly determines the absorption of light in it.

The situation is somewhat different at a wavelength of 779 nm: absorption in liver drastically increases, whereas in milk and bovine meat it decreases almost by a factor of three. Indeed, the muscle tissue is saturated with water, whereas the absorption of light by fat tissue at this wavelength is minimal [19]. Therefore, the absorption of light in muscle tissue as in milk is determined by the properties of water. On the contrary, bovine and porcine liver are saturated with blood. The absorption spectrum of deoxygenated blood has a local maximum near 779 nm [19], which mainly determines a drastic increase of absorption in liver.

The penetration depth of light into a medium is determined not only by absorption but also by scattering. The scattering coefficient depends on the sizes of particles, their shape and concentration in the medium. As the wavelength is increased, the scattering efficiency decreases. It was shown in [19, 20, 39, 40] that the scattering spectra of human biological tissues can be approximated by the empirical dependence

$$\mu_s' = a\lambda^{-b}, \tag{6}$$

where a and b are constants and $0.5 < b < 1.8$. The range of variation in the reduced scattering coefficient $6 < \mu_s' < 20\ \mathrm{cm}^{-1}$ changes weakly when the wavelength is decreased from 1064 to 779 nm. Our measurements give similar results.

Note that absorption coefficients of the bovine muscle tissue calculated in our paper coincide within the error with

the data obtained in [19] for the human muscle tissue. In this case, absorption at 1064 nm was also almost twice as large as that at 779 nm. It is difficult to compare absorption coefficients in liver with data reported in the literature because liver is strongly saturated with blood and the results of measurements will depend on the sample preparation procedure. For example, the absorption coefficient of porcine liver at 1064 nm measured in [41] is 0.1 cm^{-1}, whereas according to [42], it is equal to 2 cm^{-1}.

One of the important questions in problems of the optical and OA tomography of biological media is the choice of the laser radiation wavelength. On the one hand, light should deeply penetrate into a medium, and on the other, the difference in light absorption by healthy and diseased tissues should be maximal. Our measurements have confirmed once more that the wavelength range between 750 and 800 nm is probably optimal for solving the problems of tomography.

5. Conclusions

We have performed OA *in vitro* measurements of the in-depth distribution of laser fluence in various biological media: milk, bovine and porcine liver, and bovine muscle tissue. Experiments were carried out by using a 1064-nm Nd : YAG laser and a Ti : sapphire laser emitting at 779 nm. Two geometries for excitation and recording OA signals were considered. It was shown that the forward mode of OA signal detection yields a complete set of the optical properties of biological tissues and allows the diagnostics of the degree of their homogeneity. The backward mode of OA signal detection permits the measurement of the absorption coefficient only; however, this scheme is much more convenient and suitable for *in vivo* diagnostics of biological objects. The experimental results obtained in the paper demonstrate the applicability of the OA method for measuring laser fluence distributions in biological media and determining their optical properties.

References

1. Berlien H.P., Mueller G.J. (Eds) *Applied Laser Medicine* (Berlin: Springer-Verlag, 2003).
2. Müller G., Chance B., Alfano R. (Eds) *Medical Optical Tomography: Functional Imaging and Monitoring* (Bellingham: SPIE Press, 1993) Vol. IS11.
3. Tromberg B.J., Cerussi A., Shah N., Compton M., Fedyk A. *Breast Cancer Res.*, **7**, 279 (2005).
4. Gibson A.P., Hebden J.C., Arridge S.R. *Phys. Med. Biol.*, **50**, R1 (2005).
5. Kolkman R., Klaessens J., Hondebrink E., Hopman J., de Mul F., Steenbergen W., Thijssen J., van Leeuwen T. *Phys. Med. Biol.*, **49**, 4745 (2004).
6. Karabutov A.A., Savateeva E.V., Oraevsky A.A. *Laser Phys.*, **13**, 713 (2003).
7. Hamilton J., Buma T., Spisar M., O'Donnell M. *IEEE UFFC Trans.*, **47**, 160 (2000).
8. Paltauf G. *Proc. SPIE Int. Soc. Opt. Eng.*, **5143**, 41 (2003).
9. Kruger R.A., Kiser W.L., Reinecke D.R., Kruger G.A. *Med. Phys.*, **30**, 856 (2003).
10. Oraevsky A.A., Andreev V.G., Karabutov A.A., Esenaliev R.O. *Proc. SPIE Int. Soc. Opt. Eng.*, **3601**, 256 (1999).
11. Kozhushko V.V., Khokhlova T.D., Zharinov A.N., Pelivanov I.M., Solomatin V.S., Karabutov A.A. *J. Acoust. Soc. Am.*, **116**, 1498 (2004).
12. Tuchin V.V. *Tissue Optics: Light Scattering Methods and Instruments for Medical Diagnosis* (Bellingham, WA: SPIE Press, 2000, Vol. TT38).
13. Pham T.H., Coquoz O., Fishkin J.B., Anderson E., Tromberg B.J. *Rev. Sci. Instr.*, **71**, 2500 (2000).
14. Bevilacqua F., Berger A.J., Cerussi A.E., Jakubowski D., Tromberg B.J. *Appl. Opt.*, **39**, 6498 (2000).
15. Yang Y., Liu H., Chance B., Li X. *Opt. Eng.*, **36**, 1562 (1997).
16. Bevilacqua F., Piguet D., Marquet P., Gross J.D., Tromberg B.J., Depeursinge C. *Appl. Opt.*, **38**, 4939 (1999).
17. Kienle L., Lilge M., Patterson S., Hibst R., Steiner R., Wilson C. *Appl. Opt.*, **35**, 2304 (1996).
18. Wang R.K., Wikramasinghe Y.A. *Appl. Opt.*, **37**, 7342 (1998).
19. Pifferi A., Swartling J., Chikoidze E., Torricelli A., Taroni P., Bassi A., Andersson-Engels S., Cubeddu R. *J. Biomed. Opt.*, **9**, 1143 (2004).
20. Taroni P., Pifferi A., Torricelli A., Comelli D., Cubeddu R. *Photochem. Photobiol. Sci.*, **2**, 124 (2003).
21. Abrahamsson C., Svensson T., Svanberg S., Anderson-Engels S. *Opt. Express*, **12**, 4103 (2004).
22. Spinelli L., Torricelli A., Pifferi A., Taroni P., Danesini G.M., Cubeddu R. *J. Biomedical Opt.*, **9**, 1137 (2004).
23. Kienle A., Patterson M.S., Dognitz N., Bays R., Wagnieres G., van de Bergh H. *Appl. Opt.*, **37**, 779 (1998).
24. Wang X.J., Milner T.E., de Boer J.F., Zhang Y., Pashley D.H., Nelson J.S. *Appl. Opt.*, **38**, 2092 (1999).
25. Tearney G.J., Brezinski M.E., Southern J.F., Bouma B.E., Hee M.R., Fujimoto J.G. *Opt. Lett.*, **20**, 2258 (1995).
26. Zimnyakov D.A., Tuchin V.V. *Kvantovaya Elektron.*, **32**, 849 (2002) [*Quantum Electron.*, **32**, 849 (2002)].
27. Maslov K., Stoica G., Wang L. *Opt. Lett.*, **30**, 625 (2005).
28. Savateeva E.V., Karabutov A.A., Bell B., Johnigan R., Motamedi M., Oraevsky A.A. *Proc. SPIE Int. Soc. Opt. Eng.*, **3916**, 55 (2000).
29. Viator J.A., Paltauf G., Jaques S.L., Prahl S.A. *Proc. SPIE Int. Soc. Opt. Eng.*, **4256**, 16 (2001).
30. Khokhlova T.D., Pelivanov I.M., Kozhushko V.V., Zharinov A.N., Solomatin V.S., Karabutov A.A. *Appl. Opt.* (2006) (in press).
31. Karabutov A.A., Pelivanov I.M., Podymova N.B., Skipetrov S.E. *Kvantovaya Elektron.*, **29**, 215 (1999) [*Quantum Electron.*, **29**, 1054 (1999)].
32. Grashin P.S., Karabutov A.A., Oraevsky A.A., Pelivanov I.M., Podymova N.B., Savateeva E.V., Solomatin V.S. *Kvantovaya Elektron.*, **32**, 868 (2002) [*Quantum Electron.*, **32**, 868 (2002)].
33. *Safe Use of Lasers in Health Care Facilities*. ANSI Standard Z136.3-2005.
34. Gusev V.E., Karabutov A.A. *Lazernaya optoakustika* (Laser Opto-acoustics) (Moscow: Nauka, 1991).
35. Wang L.-H., Jacques S.L., Zheng L.-Q. *Computer Methods and Programs in Biomedicine*, **47**, 131 (1995).
36. Gardner C.M., Jacques S.L., Welch A.J. *Lasers in Surgery and Medicine*, **18**, 129 (1996).
37. Ishimaru A. *Wave Propagation and Scattering in Random Media* (New York: Academic Press, 1978; Moscow: Mir, 1981) Vols 1 and 2.
38. Karabutov A.A., Podymova N.B., Letokhov V.S. *Appl. Phys. B*, **63**, 545 (1996).

39. Karabutov A.A., Savateeva E.V., Oraevsky A.A., Podymova N.B. *J. Appl. Phys*., **87**, 2003 (2000).
40. Durduran T., Choe R., Culver J.P., Zubkov L., Holboke M.J., Giammarco J., Chance B., Yodh A.J. *Phys. Med. Biol*., **47**, 2847 (2002).
41. Cheong W.F., Prahl S.A., Welch A.J. *IEEE J. Quantum Electron*., **26**, 2166 (1990).
42. Beeky J.F., Blokland P., Posthumus P., Aalders M., Pickering J.W., Sterenborg H.J.C.M., van Gemert M.J.C. *Phys. Med. Biol*., **42**, 2255 (1997).